Nano-microstructured, superhydrophobic, and infrared transparent polytetrafluoroethylene/diamond films

Flavio Horowitz
Lívia E.V.S. Brandão
Kelly C. Camargo
Alexandre F. Michels
Naira M. Balzaretti

SPIE

Nano-microstructured, superhydrophobic, and infrared transparent polytetrafluoroethylene/diamond films

Flavio Horowitz,[a,b] Lívia E.V.S. Brandão,[b] Kelly C. Camargo,[b] Alexandre F. Michels,[c] and Naira M. Balzaretti[a,b]

[a]Universidade Federal do Rio Grande do Sul, Laser and Film Optics Laboratory/Physics Institute, Campus do Vale, Porto Alegre, Rio Grande do Sul, 91501-970 Brazil
flavio.horowitz@ufrgs.br

[b]Universidade Federal do Rio Grande do Sul, Programa de Pós-Graduação em Ciências dos Materiais, Campus do Vale, Porto Alegre, Rio Grande do Sul, 91501-970 Brazil

[c]Universidade de Caxias do Sul, Centro de Ciencias Exatas, da Natureza e de Tecnologia, Departamento de Engenharia Mecânica, Bloco D, Rua Francisco Getulio Vargas, 1130, Caxias do Sul, Rio Grande do Sul, 95070-560 Brazil

Abstract. A self-assembled polytetrafluoroethylene (PTFE) nanostructure is deposited on microcrystalline diamond (MCD) films, by use of physical and chemical vapor deposition in a two-step process, to produce (fully) superhydrophobic surfaces: high water contact angle (static, 165 ± 2 deg), very low hysteresis (dynamic, ~4 deg), and associated sliding angle (1 deg $5' \pm 15'$), thus combining the diamond infrared transparency and self-cleaning properties. These are interpreted in light of Wenzel and Cassie-Baxter wetting models, associated with structural microscopy of nano-micro rough PTFE/MCD surfaces, and present a promising perspective for self-cleaning infrared optics applications. © *2013 Society of Photo-Optical Instrumentation Engineers (SPIE)* [DOI: 10.1117/1.JNP.7.073596]

1 Introduction

Besides its extremely high hardness, wear resistance, and thermal conductance, as well as chemical inertness and biocompatibility, diamond presents a broad transmission spectrum (300 nm to 2.5 μm and 7 μm to >25 μm), which makes possible optical applications in electro-optics devices, medical instrumentation, radiation detectors, transmission windows, and domes.[1–4]

In natural bulk form, after polishing, its water contact angle (WCA), measured with a tensiometric technique, presented a slight dependence on the crystallographic planes (110) and (111), with advancing WCAs of 71 and 76 deg, respectively, and with a large angular hysteresis (H) of 47 deg (by comparison with their corresponding receding WCAs).[5] This means that it is hydrophilic (WCA < 90 deg) and that a water drop does not move easily on its surface (H > 10 deg).

In hydrogenated amorphous carbon films that were fluorinated, a-C:H:F, an opposite tendency was observed between the WCA and the friction coefficient, measured by atomic force microscopy (AFM).[6] Further incorporation of N in a-C:H:F films, motivated by the perspective of obtaining mechanical properties comparable with those of crystalline diamond, showed the same direct correlation between the friction coefficient and the WCA, in the range of 56 to 84 deg.[7] Sanchez et al. attributed these friction results to the kinetics of nucleation of the water meniscus between the moving parts; as surface hydrophobicity was increased, the water vapor condensation for the nanoscale friction process became less important. This indicates that highly hydrophobic diamond-like carbon (DLC) films are desirable for very

low-friction coefficients. As an application, DLC or fluorinated DLC coating produced significant lubrication improvement (by approximately 30%) in intravascular guidewires.[8]

On fluorine- and aluminum-doped DLC coatings, over surface topographies generated by laser-structuring and electroplating, Schulz et al.[9] obtained WCAs greater than 150 deg (static superhydrophobicity; hysteresis was not reported). Ostrovskaya et al.[10] attained large contact angles (168 ± 3 deg) for a tin melt (at 300℃ to 800℃) on nanocrystalline diamond (NCD) after hydrogen plasma treatment, but WCAs could not exceed 106 ± 4 deg at room temperature.

On NCD films, Zhou et al. achieved WCAs up to 165 deg and sliding angles smaller than 10 deg (hysteresis not reported), using surface nanostructuring by reactive ion etching and chemical modification with perfluorosilane.[11] For NCD and microcrystalline diamond (MCD), Karlsson et al.[12] reached advancing WCAs of 160 deg and 165 deg, with corresponding hysteresis values of 17 deg and 15 deg (static superhydrophobicity), respectively, by controlling termination groups with oxygen, hydrogen, and fluorine, and by a surface topography composed of pillars, produced with photolithographic resist patterning on an Al sputtered layer, later used as a mask for inductively coupled plasma etching.

Recently, Wang et al.[13] produced DLC films with WCAs up to 160 deg. Although smaller than the one mentioned above, the associated hysteresis of 11 deg is still significant, i.e., superhydrophobicity was attained in the static sense only. Moreover fabrication involved several steps: templating with a lotus leaf, replication with a polydimethylsiloxane film, Au deposition by sputtering, electrodeposition of a metallic layer, peeling off, DLC film deposition, and finally the surface was modified by perfluoropolyether adsorption.

In this first report, we dramatically reduce the number of processing steps by direct use of the as-deposited MCD films topology, followed by a self-assembled polytetrafluoroethylene (PTFE) coating nanostructure only, to produce superhydrophobic surfaces with very low hysteresis. This, combined with the diamond transmittance window in the infrared—where wavelengths are much larger than the rough surface structures involved, and thus light scattering is much smaller than otherwise, as previously reported[14]—allows for diamond-based, optical components for infrared transmission systems that are also self-cleaning.

2 Experimental

Diamond films were grown in a microwave-assisted chemical vapor deposition (CVD) reactor (MWCVD) ASTEX AX5400 (2.45 GHz). The substrates of partially stabilized zirconia, as described in a previous work,[15] 2 mm thick and with a diameter of 26 mm, were previously polished with diamond paste of 2 to 4 μm grain size. A gas mixture composed of 94% H_2 and 6% CH_4 was used, and subjected to a total pressure of 70 Torr. The microwave power was 2.5 kW, and the substrate temperature was in the range of 700℃ to 800℃. Since the diamond films, with thickness around 20 μm, did not adhere to the zirconia substrate (mechanisms involved are described in Ref. 15), both of their top (rough) and bottom (microsmooth) surfaces were available for contact angle measurements.

As in previous works,[14,16] the PTFE layer, with thickness around 120 nm, was deposited by thermal physical vapor deposition at a base pressure of 2×10^{-6} Torr. A quartz microbalance monitor was used for thickness control.

WCAs were measured using the sessile drop method by deposition of 4 to 6 μL droplets of deionized water on horizontal sample surfaces. The droplets were observed directly in cross-section with an Olympus BX-41 microscope objective lens, whereas their images were digitally captured using a 1.4-megapixel computer-controlled digital charge coupled device camera. The contact angle values were determined as averages of more than 20 measurements, performed in different areas of each sample surface. The sliding angle measurements were adjusted using a mechanical level goniometer. To determine hysteresis, advancing and receding contact angles were measured on both sides of the droplet, and in at least three different locations for each sample.

Film micro- and nanostructures were characterized by x-ray diffraction, scanning electron microscopy (SEM, EVO from Carl Zeiss), and AFM (Nanoscope IIIa from Digital Instruments, in tapping mode).

3 Results and Discussion

Surface topologies of the MCD film and of the self-assembled PTFE coating nanostructure are shown in Fig. 1.

Whereas the microsmooth side of the MCD film reproduces the substrate surface topography, including residual polishing scratches and grain boundary contours, the microroughness of the other side, shown in Fig. 1, is defined by the geometry of the diamond grains, whose size is in the range of 1 to 8 μm. Their x-ray diffraction analysis produced well-defined and narrow diffraction peaks, as seen in Fig. 2 and corresponding to the data shown in Table 1, with mostly (111) crystalline orientation.

Resulting WCAs (apparent, advancing, and receding) are illustrated in Fig. 3. From the advancing and receding angles, hysteresis (H) of the final PTFE/MCD film was around 4 deg ($H < 10$ deg, as required for dynamic superhydrophobicity).

The corresponding sliding angle, in which the water drop was in the imminence of displacement, was 1 deg $5' \pm 15'$ (uncertainty due to the horizontal line positioning; that of the goniometer reading was $\pm 1'$). Besides the final WCAs, intermediary values for both rough and microsmooth faces are shown in Table 2.

The apparent WCA for the MCD rough surface, θ_d can be interpreted in terms of the Cassie-Baxter model, in which the water drop has interfaces with the topology of the solid surface as well as with its trapped air, by taking into account the liquid–solid surface area (SA) fraction, f_s, and the liquid–air SA fraction, f_a, through the relation[19]

$$\cos \theta_d = f_s \cos \theta_y - f_a, \qquad f_s + f_a = 1, \tag{1}$$

where θ_y is Young's angle (i.e., the apparent contact angle on a perfectly smooth plane). Since this angle is approximately the WCA measured on the MCD surface that was facing the zirconia substrate during film deposition, listed in Table 2 as MCD microsmooth surface, $f_s = 78.55\%$
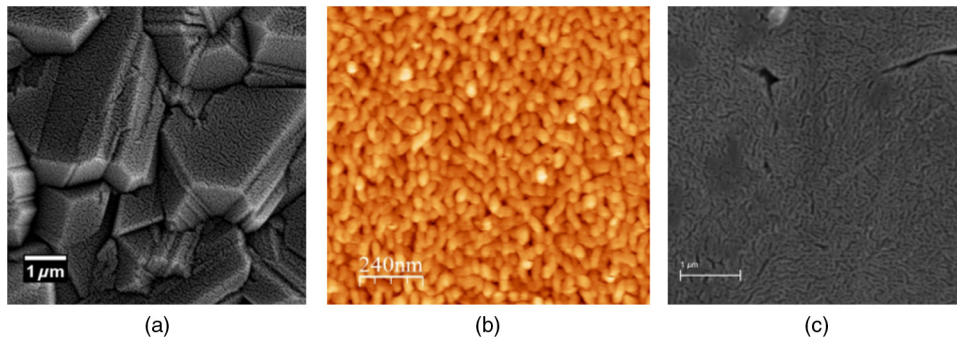

Fig. 1 Multiscale topologies of the PTFE/MCD film: (a) micro-nano rough side (SEM, 1 μm scale bar); (b) close-up of rough side with PTFE overlayer (AFM, 240 nm scale bar); and (c) microsmooth side (SEM, 1 μm scale bar).
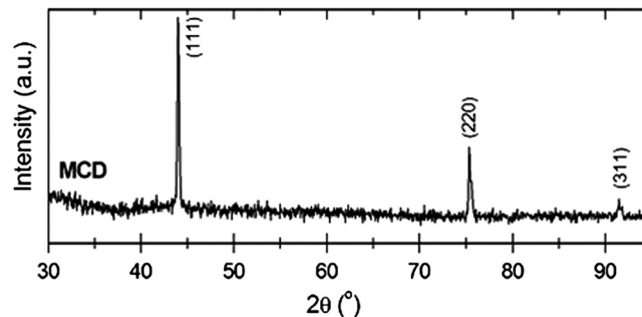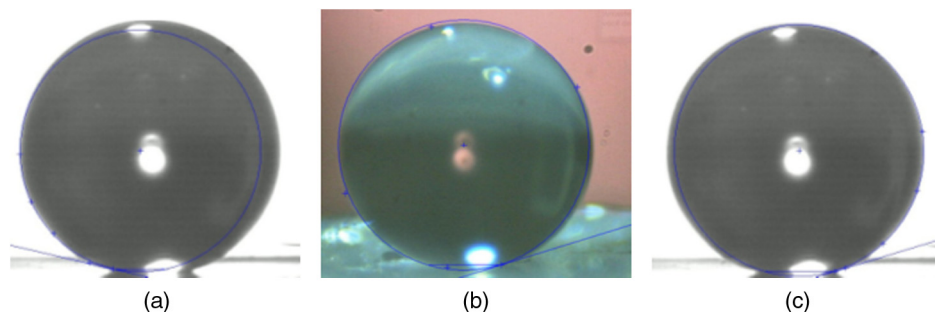

Fig. 2 X-ray diffraction patterns of MCD films.

Table 1 MCD film data obtained from x-ray diffraction.

(hkl)	2θ (deg)	Full width at half maximum (deg)	I/I (111)
(111)	44.026 ± 0.001	0.157 ± 0.002	1.0
(220)	75.40 ± 0.01	0.17 ± 0.03	0.3
(311)	91.53 ± 0.04	0.4 ± 0.1	<0.1

(a)	(b)	(c)

Fig. 3 Water contact angles of PTFE/MCD rough film: (a) advancing of 167 ± 2 deg; (b) apparent of 165 ± 2 deg; and (c) receding of 163 ± 2 deg, where their determination lines are shown.

Table 2 Water contact angles: Reference and measured values in this work.

Sample description	WCA
Polycrystalline diamond films with oxygen termination[17]	32 deg
Polycrystalline diamond films with hydrogen termination[18]	93 deg
Smooth PTFE	109 deg
MCD microsmooth surface (this work)	92 ± 2 deg
MCD rough surface (this work)	104 ± 2 deg
PTFE over MCD microsmooth surface (this work)	127 ± 2 deg
PTFE over MCD rough surface (this work)	165 ± 2 deg

and $f_a = 21.45\%$ are good estimates, making evidence of the rough MCD topology contribution through air trapping.

However, the Wenzel model is more appropriate for the PTFE overlayer, since it is completely immersed in water due to its thinness, and thus the rough surface WCA, θ_r, is such that[20]

$$\cos \theta_d = r \cos \theta_o \qquad r = \text{SA/projected SA}, \qquad (2)$$

where θ_o is the MCD microsmooth surface WCA, also listed in Table 1. The roughness factor $r = 1.85$ follows.

Furthermore, the solid that interfaces with water, instead of the MCD in the previous case, now becomes the PTFE overlayer with a much lower surface energy along the SA, which is increased by 85% through the nanoroughness estimated above. These are the chemical and physical reasons for the WCA enhancement promoted by the PTFE on the MCD rough surface, and the same applies for the PTFE-driven hydrophobicity improvement of the microsmooth surface.

4 Conclusions

A first report was presented on PTFE-coated MCD films, requiring a two-step preparation procedure, much simpler than previous, to attain a high WCA (165 ± 2 deg). This was interpreted with Wenzel and Cassie-Baxter wetting models to allow understanding of the role of the physical MCD microroughness and of the PTFE nanoroughness, besides that of the chemical surface energy.

In addition, the PTFE/MCD nano-micro rough surface, to this date and to our best knowledge, provided the lowest reported hysteresis value of ~4 deg, which accounts for the dynamic aspect of superhydrophobicity, for a diamond or diamond-like carbon film.

Combination of the resulting superhydrophobicity with the well-known diamond transparency window in the infrared (above 7 μm), whereas the PTFE overlayer with nanometric thickness and roughness presents very low transmission loss, allows application for several self-cleaning optical components, such as windows for CO_2 lasers, night vision cameras, infrared detectors, as well as for portable equipment, such as infrared spectrophotometers, used in the field for analysis of environmental contaminants.

Acknowledgments

References

1. J. C. Angus, "Emerging CVD science and technology," Chapter 2 in *Synthetic Diamond*, K. E.Spear and J. P. Dismukes, Eds., pp. 21–40, Wiley, New York (1994).
2. F. G. Celii and J. E. Butler, "Diamond chemical vapor-deposition," *Ann. Rev. Phys. Chem.* **42**, 643–684 (1991), http://dx.doi.org/10.1146/annurev.pc.42.100191.003235.
3. G. M. Swain, "The susceptibility to surface corrosion in acidic fluoride media: a comparison of diamond, HOPG, and glassy carbon electrodes," *J. Electrochem. Soc.* **141**(12), 3382–3393 (1994), http://dx.doi.org/10.1149/1.2059343.
4. M. Schwander and K. Partes, "A review of diamond synthesis by CVD processes," *Diam. Relat. Mater.* **20**(9), 1287–1301 (2011), http://dx.doi.org/10.1016/j.diamond.2011.08.005.
5. J. O. Hansen et al., "A tensiometric study of diamond (111) and (110) fases," *J. Coll. Inter. Sci.* **130**(2), 347–358 (1989), http://dx.doi.org/10.1016/0021-9797(89)90114-8.
6. R. Prioli et al., "Nanotribological properties of amorphous carbon-fluorine films," *Tribol. Lett.* **15**(3), 177–180 (2003), http://dx.doi.org/10.1023/A:1024848816646.
7. C. M. T. Sanchez et al., "Nitrogen incorporation into hard fluorinated carbon films: nanoscale friction and structural modifications," *Diam. Relat. Mater.* **13**(4–8), 1366–1370 (2004), http://dx.doi.org/10.1016/j.diamond.2003.10.062; E. Riedo, F. Levy, and H. Brune, "Kinetics of capillary condensation in nanoscopic sliding friction," *Phys. Rev. Lett.* **88**(18), 185505 (2002), http://dx.doi.org/10.1103/PhysRevLett.88.185505.
8. T. Hasebe et al., "Lubrication performance of diamond-like carbon and fluorinated diamond-like carbon coatings for intravascular guidewires," *Diam. Relat. Mater.* **15**(1), 129–132 (2006), http://dx.doi.org/10.1016/j.diamond.2005.08.025.
9. H. Schulz et al., "Ultra hydrophobic wetting behaviour of amorphous carbon films," *Surf. Coat. Technol.* **200**(1–4), 1123–1126 (2005), http://dx.doi.org/10.1016/j.surfcoat.2005.02.019.
10. L. Ostrovskaya et al., "Wettability of nanocrystalline diamond films," *Diam. Relat. Mater.* **16**(12), 2109–2113 (2007), http://dx.doi.org/10.1016/j.diamond.2007.07.026.

11. Y. B. Zhou et al., "Preparation of superhydrophobic nanodiamond and cubic boron nitride films," *Appl. Phys. Lett.* **97**(13), 133110 (2010), http://dx.doi.org/10.1063/1.3494269.

12. M. Karlsson, P. Forsberg, and F. Nikolajeff, "From hydrophilic to superhydrophobic: fabrication of micrometer-sized nail-head-shaped pillars in diamond," *Langmuir* **26**(2), 889–893 (2010), http://dx.doi.org/10.1021/la902361c.

13. Y. Wang et al., "From natural lotus leaf to highly hard-flexible diamond-like carbon surface with superhydrophobic and good tribological performance," *Surf. Coat. Technol.* **206**(8–9), 2258–2264 (2012), http://dx.doi.org/10.1016/j.surfcoat.2011.10.001.

14. K. C. Camargo et al., "Multi-scale structured, superhydrophobic and wide-angle, antireflective coating in the near-infrared region," *Chem. Commun.* **48**(41), 4992–4994 (2012), http://dx.doi.org/10.1039/c2cc30456b; M. F. Kuhn, "Visible and near infrared, wide-angle, antireflection coatings with self-cleaning on glass," *Opt. Mat. Express* **2**(7), 969–977 (2012), http://dx.doi.org/10.1364/OME.2.000969.

15. M. M. Lucchese et al., "Partially stabilized zirconia substrate for chemical vapor deposition of free-standing diamond films," *Diam. Relat. Mater.* **14**(10), 1605–1610 (2005), http://dx.doi.org/10.1016/j.diamond.2005.04.012.

16. A. F. Feil et al., "Micro and nano-texturization of intermetallic oxide alloys by a single anodization step: preparation of artificial self-cleaning surfaces," *ACS Appl. Mater. Interf.* **3**(10), 3981–3987 (2011), http://dx.doi.org/10.1021/am200854r; D. E. Weibel et al., "Adjustable hydrophobicity of Al substrates by chemical surface functionalization of nano/microstructures," *J. Phys. Chem. C* **114**(31), 13219–13225 (2010), http://dx.doi.org/10.1021/jp103702d; D. Goswami, S. K. Medda, and G. De, "Superhydrophobic films on glass surface derived from trimethylsilanized silica gel nanoparticles," *ACS Appl. Mater. Sci.* **3**(9), 3440–3447 (2011), http://dx.doi.org/10.1021/am200666m.

17. L. Y. Ostrovskaya, "Studies of diamond and diamond-like film surfaces using XAES, AFM and wetting," *Vacuum* **68**(3), 219–238 (2002), http://dx.doi.org/10.1016/S0042-207X(02)00460-8.

18. Z. Q. Yao et al., "Structural, mechanical and hydrophobic properties of fluorine-doped diamond-like carbon films synthesized by plasma immersion ion implantation and deposition (PIII-D)," *Appl. Surf. Sci*. **230**(1–4), 172–178 (2004), http://dx.doi.org/10.1016/j.apsusc.2004.02.044.

19. A. B. D. Cassie and S. Baxter, "Wettability of porous surfaces," *Trans. Faraday Soc.* **40**, 546–551 (1944), http://dx.doi.org/10.1039/tf9444000546.

20. R. N. Wenzel, "Surface roughness and contact angle," *J. Phys. Chem.* **53**(9), 1466–1467 (1949), http://dx.doi.org/10.1021/j150474a015.

Flavio Horowitz obtained his PhD in optical sciences from University of Arizona, Tucson, in 1983 and postdoctorate in optical semiconductor devices from Imperial College, London, in 1993. He is presently an associate professor of physics at Universidade Federal do Rio Grande do Sul (UFRGS, Porto Alegre, Brazil), CNPq level 1 researcher and leader of the Laser and Film Optics Laboratory. His research interests include monitored manufacturing of optical coatings, micro-nanostructured films, superhydrophobicity, and optical materials with regard to optical devices.

Lívia E.V.S. Brandão has a bachelor's degree in physics and a master's degree in materials science from UFRGS, Brazil. She is now in a joint doctorate program on CVD nanodiamonds between UFRGS and Institut Néel, Université Joseph Fourier, Grenoble I (France). She has mainly worked with carbonaceous materials and analysis techniques, such as Raman spectroscopy, x-ray diffraction, scanning electron microscopy, transmission electron microscopy, and focused ion beam.

Kelly C. Camargo holds a postdoctoral position in the Institut Lumière Matière, Université LYON 1, France. She received her PhD degree in physics from UFRGS, Brazil, in 2012. Her research interests include the study of optical coatings and wettability, with emphasis on superhydrophobic/self-cleaning surfaces.

Alexandre F. Michels obtained his MSc in engineering in 1999 and his PhD in materials science in 2004 from Universidade do Rio Grande do Sul. He has developed, during his postdoctoral research, superhydrophobic surfaces by nanostructuring. He has experience in real-time optical monitoring, interferometry and polarimetric metrology, laser viscometry, thin film production by physical vapor deposition, dip and spin coating, characterization of sol-gel films, and superhydrophobic surfaces. He is currently adjunct professor in the Center for Science and Technology of Universidade de Caxias do Sul.

Naira M. Balzaretti, PhD, is an associate professor in the Physics Department at Federal University of Rio Grande do Sul, Brazil. Her research fields of interest are related to materials science, focused in CVD diamond deposition, high-pressure and high-temperature processing, Raman spectroscopy, nanocarbon and ceramic materials.